Supporting Information

Bismuth telluride-copper telluride nanocomposites from heterostructured building blocks

Yu Zhang,[a] Yu Liu,[a,b]* Mariano Calcabrini,[b] Congcong Xing,[a] Xu Han, [c] Jordi Arbiol,[c,d] Doris Cadavid,[e] Maria Ibáñez,[b] and Andreu Cabot[a,d]*

a. Catalonia Energy Research Institute - IREC, Sant Adria de Besòs, 08930 Barcelona, Spain.
b. IST Austria, Am Campus 1, 3400 Klosterneuburg, Austria.
c. Catalan Institute of Nanoscience and Nanotechnology (ICN2), CSIC and BIST, Campus UAB, Bellaterra, 08193 Barcelona, Catalonia, Spain.
d. ICREA, Pg. Lluis Companys 23, 08010 Barcelona, Catalonia, Spain
e. Departamento de Fisica, Universidad Nacional de Colombia 111321, Ciudad Universitaria, Bogota, Colombia

* *E-mails:*
Y. Liu: *yu.liu@ist.ac.at*
A. Cabot: *acabot@irec.cat*

Contents

1. Additional structural characterization of Bi_2Te_3-$Cu_{2-x}Te$ nanowires.

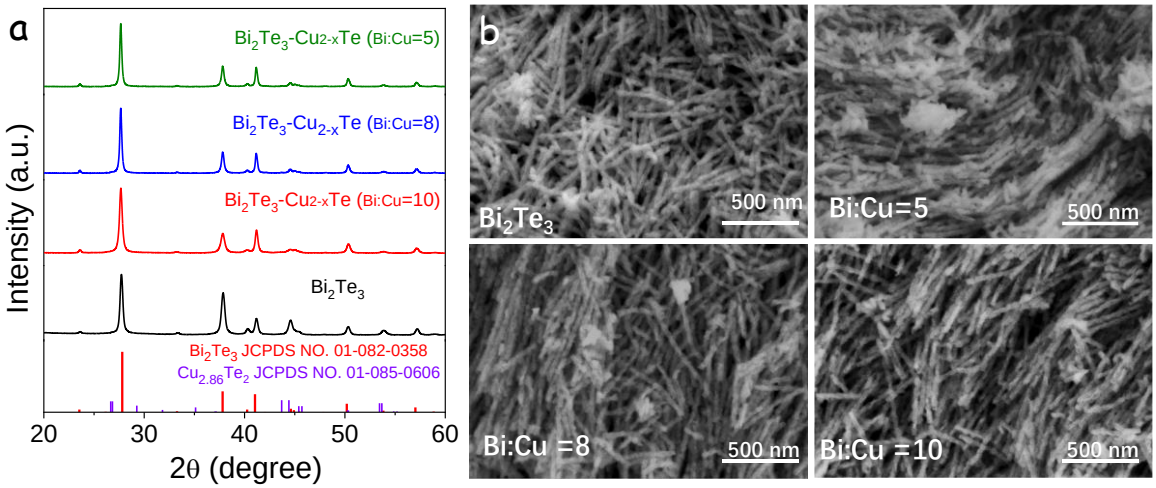

Figure S1. (a) XRD patterns of Bi_2Te_3-$Cu_{2-x}Te$ nanowires. (b) Representative SEM micrographs of Bi_2T_3-$Cu_{2-x}Te$ nanowires, Bi_2Te_3. Bi_2Te_3-$Cu_{2-x}Te$ (Bi:Cu=5), Bi_2Te_3-$Cu_{2-x}Te$ (Bi:Cu=8) and Bi_2Te_3-$Cu_{2-x}Te$ (Bi:Cu=10), as indicated in each image.

2. Additional characterization of consolidated composites.

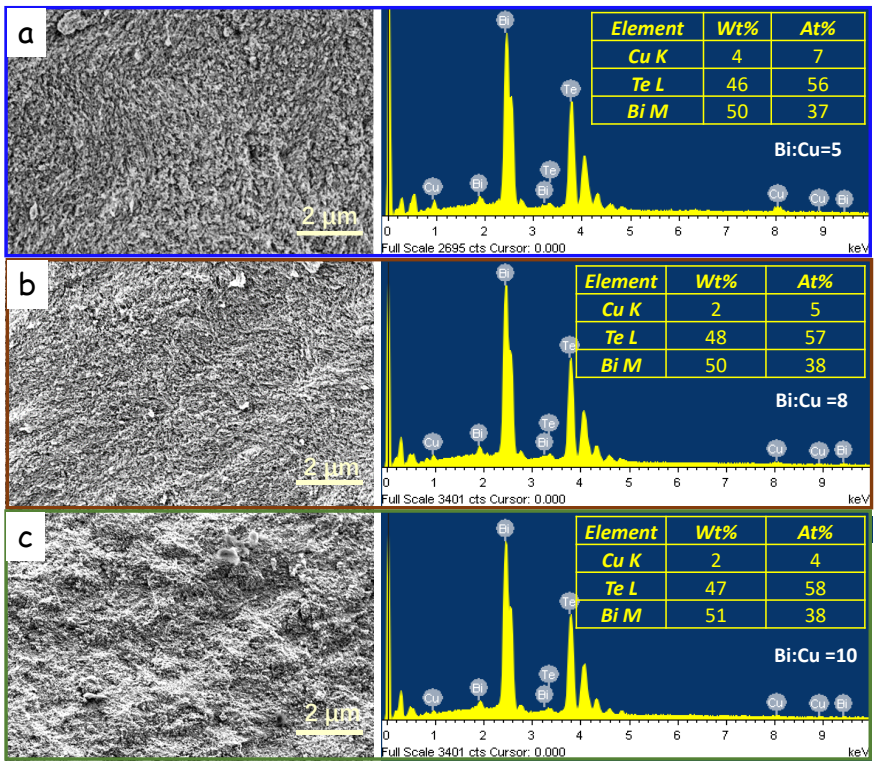

Figure S2. SEM image, EDX pattern and composition of Bi_2Te_3-$Cu_{2-x}Te$ pellets. (a) Bi_2Te_3-$Cu_{2-x}Te$ (Bi:Cu=5), (b) Bi_2Te_3-$Cu_{2-x}Te$ (Bi:Cu=8) and (c) Bi_2Te_3-$Cu_{2-x}Te$ (Bi:Cu=10), respectively.

Table S1. Density of hot pressed Bi_2Te_3 and Bi_2Te_3-$Cu_{2-x}Te$ samples.

Sample	Density (g/cm^3)	Relative Density
Bi_2Te_3	6.63	86.1%
Bi_2Te_3-$Cu_{2-x}Te$ (Bi:Cu =10)	6.59	86.7%
Bi_2Te_3-$Cu_{2-x}Te$ (Bi:Cu =8)	6.54	87.2%
Bi_2Te_3-$Cu_{2-x}Te$ (Bi:Cu =5)	6.44	87.0%

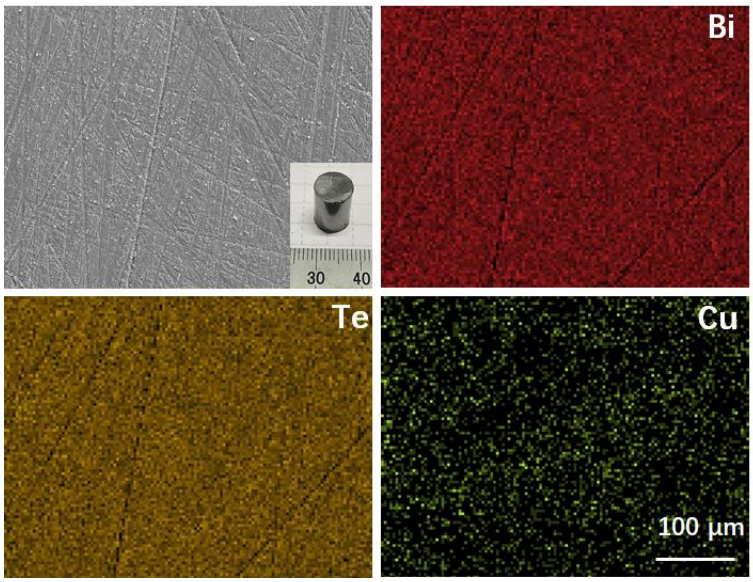

Figure S3. SEM micrograph of a Bi_2Te_3-$Cu_{2-x}Te$ (Bi:Cu=10) pellet and corresponding EDX elemental maps.

3. Anisotropy characterization.

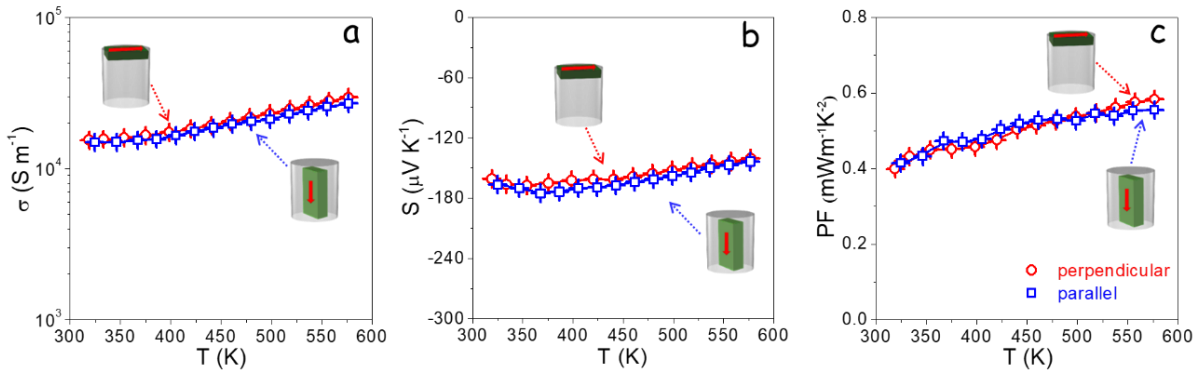

Figure S4. Temperature dependence of thermoelectric properties of Bi_2Te_3-$Cu_{2-x}Te$ (Bi:Cu=8) in two directions, perpendicular (red) and parallel (blue) to the pressure axis, as marked within the graphs: (a) electric conductivity, σ; (b) Seebeck coefficient, S; (c) power factor or $S^2\sigma$, PF.

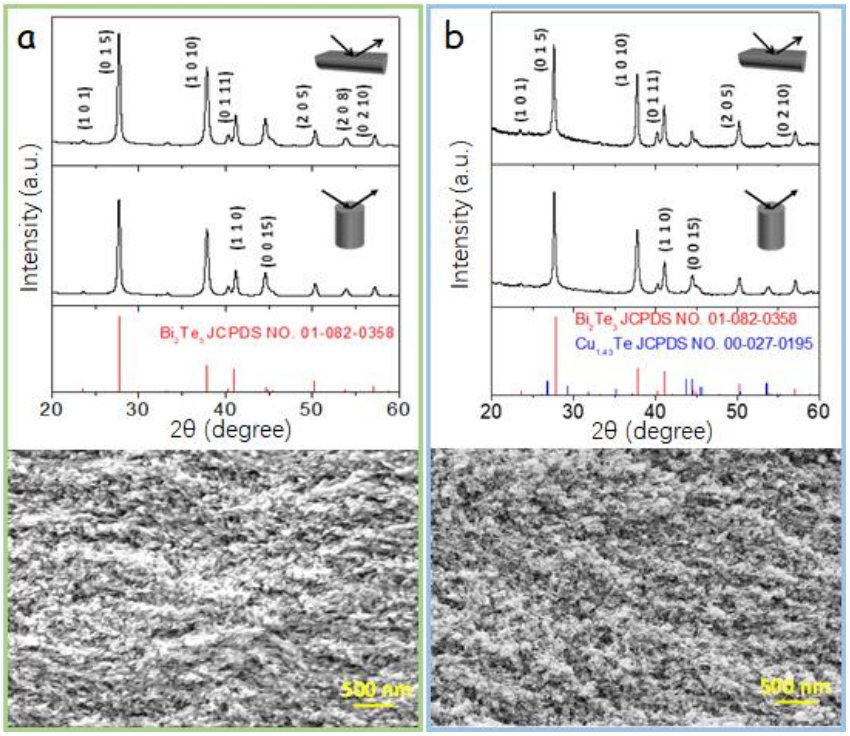

Figure S5. XRD pattern and SEM micrographs of consolidated pellets in two normal directions, perpendicular and parallel to the pressure axis, as marked within the graphs. (a) Bi_2Te_3 and (b) Bi_2Te_3-$Cu_{2-x}Te$ (Bi:Cu=8).

4. TE properties of Bi_2Te_3-$Cu_{2-x}Te$ pellet with different annealing temperature.

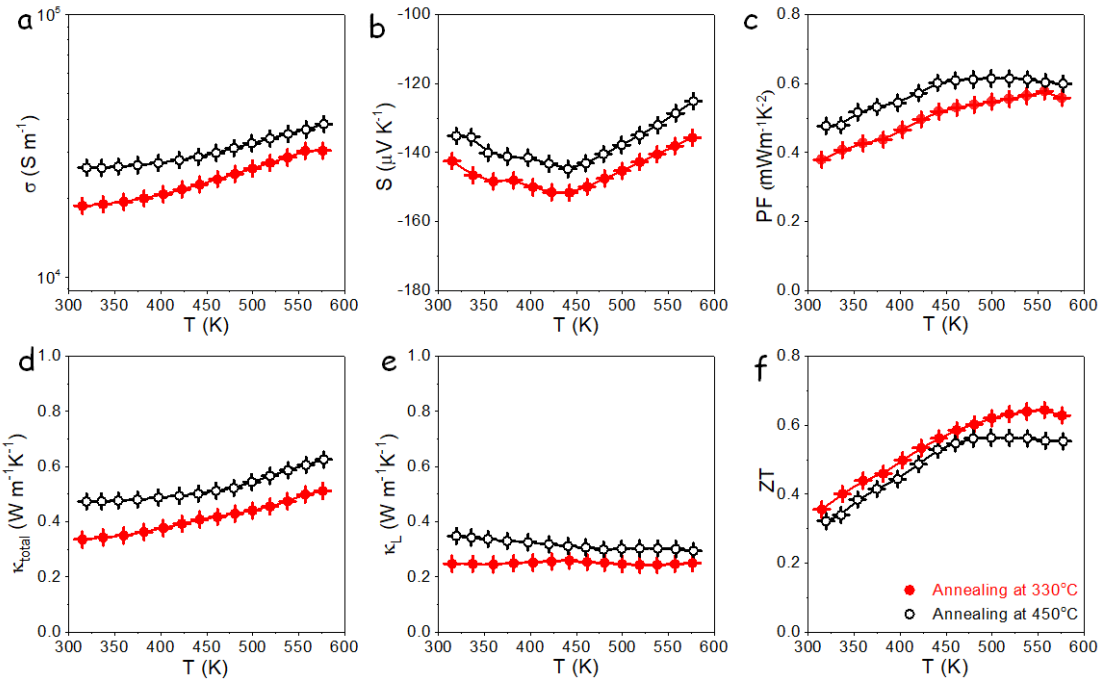

Figure S6. Temperature dependence of thermoelectric properties of Bi_2Te_3-$Cu_{2-x}Te$ (Bi:Cu=8) sample annealed at 330 °C (solid symbols) and 450 °C (open symbols) respectively: (a) electric conductivity, σ; (b) Seebeck coefficient, S; (c) power factor or $S^2\sigma$, PF; (d) total thermal conductivity, κ_{total}; (e) lattice thermal conductivity; (f) TE figure of merit, ZT.

5. Electronic thermal conductivity, porosity correction and Cahill limit.

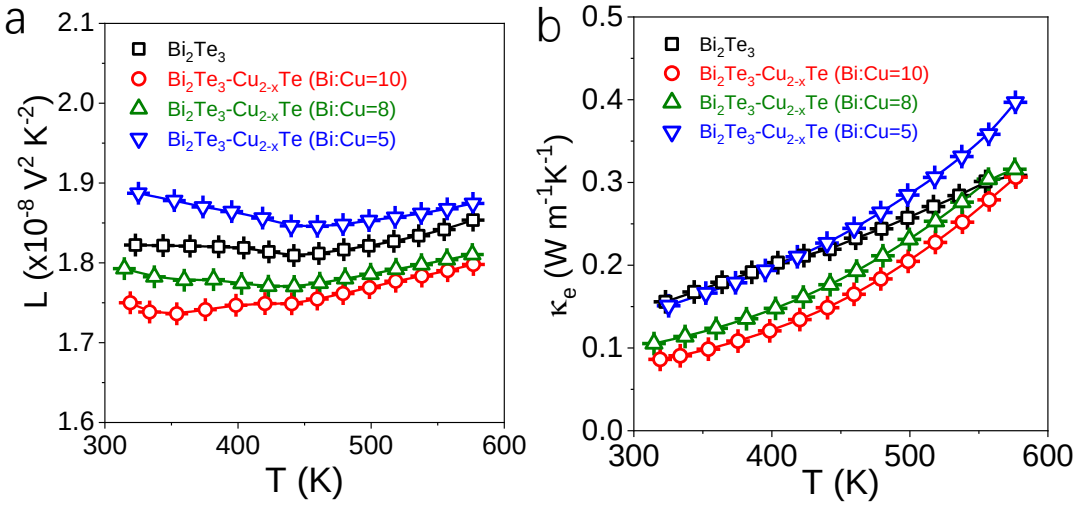

Figure S7. Temperature dependence of (a) Lorentz number (L) and (b) electronic thermal conductivity (κ_e) of Bi_2Te_3 and Bi_2Te_3-$Cu_{2-x}Te$ pellets.

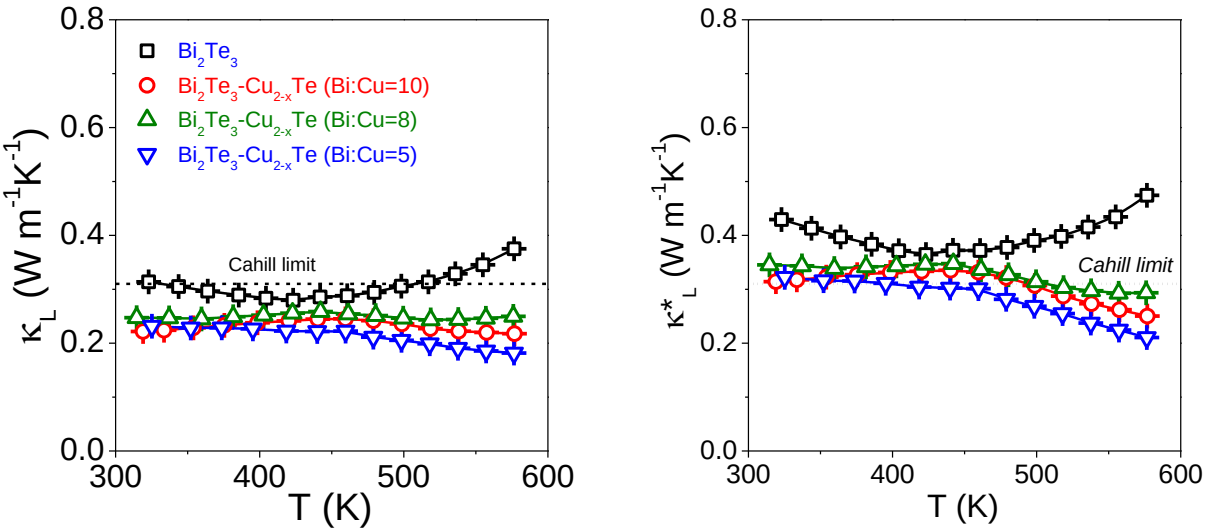

Figure S8. Lattice thermal conductivity before (felt) and after (right) porosity correction and including the Cahill limit estimated for pure Bi_2Te_3 at ambient temperature (0.31 $Wm^{-1}K^{-1}$).[1]

The porosity contribution to the thermal conductivity was estimated from Maxwell-Eucken equation.[2,3]

$$\zeta_{100} = \zeta_P \frac{1+\beta P}{1-P}$$

Where ζ_{100} is the thermal conductivity in 100 % dense medium, P is the porosity degree in the range between 0 and 1, β is an empirical parameter related to the pore geometry, which we fixed to 2.[4] A correction factor of 1.5 was obtained when taking account the 86-87 % relative density of our samples. So the lattice thermal conductivities of 100% densified pellet in our work were estimated within range of 0.32 $Wm^{-1}K^{-1}$ (Bi_2Te_3-$Cu_{2-x}Te$) ~ 0.44 $Wm^{-1}K^{-1}$ (Bi_2Te_3), which are slightly higher than Cahill limit (0.31 $Wm^{-1}K^{-1}$).

6. Phonon modeling studies.

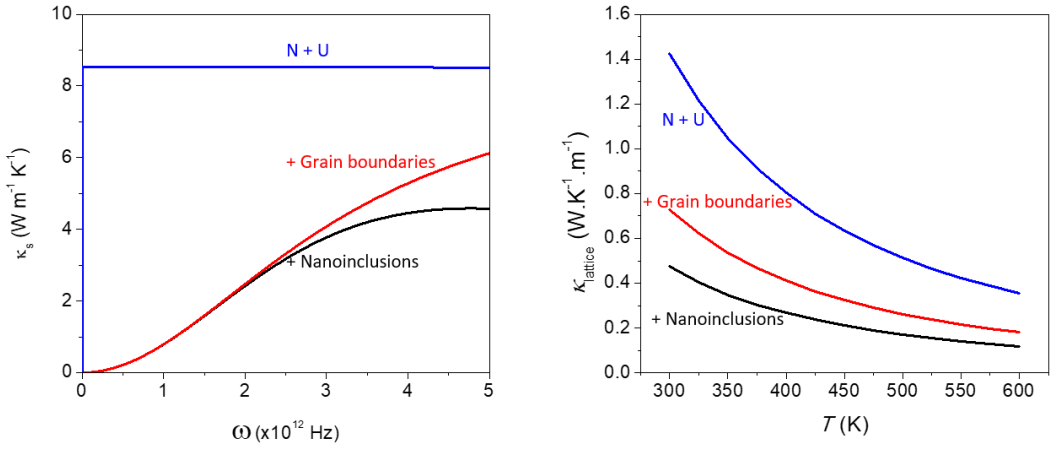

Figure S9. Calculated spectral lattice conductivity at 600 K (a) and thermal lattice conductivity (b) for a sample of Bi_2Te_3-$Cu_{2-x}Te$ (Bi:Cu =10). The calculated values are in accordance with our measurements for pristine Bi_2Te_3 (red curves, when nanoinclusions are not considered) and for Bi_2Te_3-$Cu_{2-x}Te$ (black curves). The higher values of calculated thermal conductivities with respect to the measured ones are an effect of the high porosity of the samples.

We calculated the thermal lattice conductivity, κ_l, with the Debye-Callaway model from the total phonon relaxation time τ_{tot}:[5, 6]

$$\kappa_l = \frac{\kappa_B}{2\pi^2 \upsilon}\left(\frac{\kappa_B T}{\hbar}\right)^3 \int_0^{\frac{\theta_D}{T}} \tau_{tot} \frac{z^4 \exp(z)}{[\exp(z)-1]^2} dz \qquad \text{(S1)}$$

The integrand together with the coefficient in Eq. (S1) is the spectral lattice thermal conductivity, κ_s,[3] and reports which phonon frequencies contribute more to the thermal conductivity at a particular temperature:

$$\kappa_s = \frac{\kappa_B}{2\pi^2 \upsilon}\left(\frac{\kappa_B T}{\hbar}\right)^7 \tau_{tot} \frac{z^4 \exp(z)}{[\exp(z)-1]^2} \qquad \text{(S2)}$$

In the above equations, $z = \frac{\hbar\omega}{\kappa_B T}$ is the reduced phonon frequency, $\hbar$ is the reduced Plank constant, $\upsilon = \left[\frac{1}{3}\left(\frac{1}{\upsilon_L^3} + \frac{2}{\upsilon_T^3}\right)\right]^{-1/3}$ is the average sound velocity (with υ_L and υ_T denoting the longitudinal and shear sound velocities respectively) and θ_D is the Debye temperature calculated as $\frac{\hbar}{2\pi\kappa_B}\left(\frac{3N}{4\pi V}\right)^{1/3}\upsilon$, where N is the number of atoms a the unit cell and V its volume.

The total phonon relaxation time is calculated for different scattering mechanisms. The most common ones are Normal (N) and Umklapp (U) phonon-phonon scattering and grain boundary scattering (GB).[8] In addition we included nanoprecipitates (NP) as a source of phonon scattering in our calculations.[9]

The different phonon relaxation times were calculated as follows:

Umklapp phonon scattering rate:

$$\tau_U^{-1} = \frac{\hbar\gamma^2\omega^2 T}{\bar{M}v^2\theta_D} exp\left(-\frac{\theta_D}{3T}\right) \quad (S3)$$

Normal process scattering rate:

$$\tau_N^{-1} = \beta\tau_U^{-1} \quad (S4)$$

Grain boundary scattering rate:

$$\tau_{GB}^{-1} = \frac{v}{d} \quad (S5)$$

Nanoprecipitates phonon scattering rate:

$$\tau_{NP}^{-1} = v\left[(2\pi R^2)^{-1} + \left(\pi R^2 \frac{4}{9}\left(\frac{\Delta D}{D}\right)^2 \left(\frac{\omega R}{v}\right)^4\right)^{-1}\right]^{-1} N_p \quad (S6)$$

To consider multiple scattering mechanisms simultaneously, the scattering rates (τ^{-1}) are added according to Matthiessen's rule:

$$\tau_{tot}^{-1} = \sum_{Mechanisms} \tau_i^{-1} \quad (S7)$$

In the above equations, γ is the Grüneisen parameter, β a fitted ratio between Normal and Umklapp processes, $\bar{V} = V/N$ the average atomic volume, $\bar{M}$ the average atomic mass, d the grain size, a the lattice parameter, R the average radius for the precipitates, D the matrix density, ΔD is density difference between the precipitate and matrix, and N_p the number density of precipitates.

In the calculations we used parameters from a Bi_2Te_3-Cu_{2-x} Te (Bi:Cu =10) sample. The nanoprecipitate density was estimated from the radius and the ratio Bi:Cu.

Table S2. Parameters used to calculate κ_l and κ_s

Parameters	values
Longitudinal Sound Velocity	2800 m s^{-1}
Transverse Sound Velocity	1600 m s^{-1}
Grüneisen Parameter	1.5
Average Atomic Mass	160.15
Average Atomic Volume	34.8 $Å^3$
Average Lattice Parameter	6.73 Å

Ratio Normal to Umklapp	2.8 (fitted)
Debye Temperature	162.1 K (calculated)
Matrix Density	7.6 $g.cm^{-3}$
Precipitate Density	7.27 $g.cm^{-3}$
Nanoprecipitate Density	2×10^{23} m^{-3}
Nanoprecipitate Radius	3 nm
Grain size	50 nm

The relatively higher values of thermal conductivities obtained in the calculations in comparison with the measured ones is an effect of the porosity of the pellets. For samples with densities of ~87% the porosity correction factor is around 1.3 meaning that materials with the theoretical maximum density will have thermal conductivities 30% higher.[2,3]

7. References.

(1) C. Chiritescu, C. Mortensen, D. G. Cahill, *J. Appl. Phys*. 2009, **106**: 073503.
(2) L. Yang, J. Wu, L. T. Zhang, *J. Alloys Compd.* 2004, **364**: 83-88.
(3) M. Ibáñez, R. Korkosz, Z. Luo, P. Riba, D. Cadavid, S. Ortega, A. Cabot, Kanatzidis, M, *J. Am. Chem. Soc.* 2015, **137**: 4046-4049.
(4) J. Adachi, K. Kurosaki, M. Uno, *J. Alloys Compd.* 2007, **432**: 7-10.
(5) J. Callaway, B. Von, *Phys. Rev.* 1960, **120**, 1149–1154.
(6) D. Bessas, I. Sergueev, H.C. Wille, J. Peron, D. Ebling, Matter *Mater. Phys.* 2012, **86**, 224301.
(7) T.J. Zhu, F.G. Fu, H.H. Xie, Y.T. Liu, B. Feng, J. Xie, X.B. Zhao, *Epl* 2013, **104**, 46003.
(8) H. Xie, H. Wang, Y. Pei, C. Fu, X. Liu, G.J. Snyder, X. Zhao, T. Zhu, *Adv. Funct. Mater.* 2013, **23**, 5123–5130.
(9) B. Singh, V.J. Menon, K.C. Sood, *Matter Mater. Phys.* 2006, **74**, 184302.